



# Comparative toxicity of ultrafine particles around a major airport in human bronchial epithelial (Calu-3) cell model at the air–liquid interface

Rui-Wen He<sup>a,b</sup>, Miriam E. Gerlofs-Nijland<sup>a</sup>, John Boere<sup>a</sup>, Paul Fokkens<sup>a</sup>, Daan Leseman<sup>a</sup>,  
Nicole A.H. Janssen<sup>a</sup>, Flemming R. Cassee<sup>a,b,\*</sup>

<sup>a</sup> National Institute for Public Health and the Environment (RIVM), P.O. Box, 3720, BA, Bilthoven, the Netherlands

<sup>b</sup> Institute for Risk Assessment Sciences, Utrecht University, P.O. Box 80178, 3508, TD, Utrecht, the Netherlands

## ARTICLE INFO

### Keywords:

UFPs  
Airport emission  
Road traffic emission  
Calu-3 cell  
Air–liquid interface  
BMD analysis

## ABSTRACT

Relatively high concentrations of ultrafine particles (UFPs) have been observed around airports, in which aviation and road traffic emissions are the major sources. This raises concerns about the potential health impacts of airport UFPs, particularly in comparison to those emitted by road traffic. UFPs mainly derived from aviation or road traffic emissions were collected from a location near a major international airport, Amsterdam-Schiphol airport (AMS), depending on the wind direction, along with UFPs from an aircraft turbine engine at low and full thrust. Human bronchial epithelial cells (Calu-3) model in combination with an air–liquid interface (ALI) cloud system was used for the in vitro exposure to UFPs at low doses ranging from 0.09 to 2.07  $\mu\text{g}/\text{cm}^2$ . Particle size distribution was measured. Cell viability, cytotoxicity and inflammatory potential (interleukin (IL) 6 and 8 secretion) on Calu-3 cells were assessed after exposure for 24 h. The biological measurements on Calu-3 cells confirm that pro-inflammatory responses still can be activated at the high cell viability (> 80%) and low cytotoxicity. By the Benchmark Dose (BMD) analysis, Airport and Non-Airport (road traffic) UFPs as well as UFPs samples from a turbine engine have similar toxic properties. Our results suggest that UFPs from aviation and road traffic in airport surroundings may have similar adverse effects on public health.

## 1. Introduction

Relatively high concentrations of ultrafine particles (UFPs, particle size < 100 nm), expressed as number per volume, have been observed around airports primarily linked with aviation activities (Hudda and Fruin, 2016; Keuken et al., 2015; Masiol and Harrison, 2014; Ren et al., 2018; Riley et al., 2016; Winther et al., 2015). Although characteristics (e.g. size distribution) and sources of the airport UFPs are becoming clear (Stacey, 2019), little is known about their toxicity as well as the comparison of their toxicity with UFPs from other sources such as road traffic.

Large airports are usually surrounded by major motorways. Consequently, aviation activity and road traffic are the major sources to the particles in airport surroundings (He et al., 2018). A recent study reported total particles number concentrations (PNCs) of around 35,000 particles/ $\text{cm}^3$  at a monitoring site nearby the Amsterdam-Schiphol airport (AMS, the Netherlands), in which aviation activity was estimated to account for 79% and road traffic for 18% of PNCs (Pirhadi et al., 2020). Aircraft emissions are characterized by a smaller particle size compared to other combustion sources, such as road traffic (Stacey,

2019). The small class of UFPs contributes mostly to the size distribution for aviation emissions with a strong increase in the range of 10–20 nm, while the size of UFPs from road traffic is generally larger than 50 nm (Keuken et al., 2015; Pirhadi et al., 2020; Shirmohammadi et al., 2017). The size of particles is an important characteristic, which can influence not only their toxic potency, but also where particles exert their toxicity (Heusinkveld et al., 2016; Miller et al., 2017; Stone et al., 2017; Terzano et al., 2010). Depending on the size distribution of UFPs, the exposure risks may differ. Therefore, understanding the associated risks due to exposure to UFPs from aviation and road traffic emissions is of great significance to gain better insight into the extent of their contributions to health effects.

To better assess the potential toxicity of inhaled UFPs, the air–liquid–interface (ALI) exposure via exposure systems was developed. Compared to the traditional in vitro exposure by adding the particles suspension into medium, ALI exposure allows particles to be deposited on semi-dry apical cell surface via a continuous flow or single cloud to adequately resemble the realistic inhalation exposure in lungs (BéruBé et al., 2010; Kim et al., 2016), thereby being applicable in many toxicity studies (Antherieu et al., 2017; Fizeşan et al., 2019; Mühlhopt et al.,

\* Corresponding author at: Institute for Risk Assessment Sciences, Utrecht University, P.O. Box 80178, 3508, TD, Utrecht, the Netherlands

E-mail address: [flemming.cassee@rivm.nl](mailto:flemming.cassee@rivm.nl) (F.R. Cassee).

<https://doi.org/10.1016/j.tiv.2020.104950>

Received 8 May 2020; Received in revised form 17 July 2020; Accepted 22 July 2020

Available online 26 July 2020

0887-2333/ © 2020 The Author(s). Published by Elsevier Ltd. This is an open access article under the CC BY-NC-ND license (<http://creativecommons.org/licenses/by-nc-nd/4.0/>).

2016). UFPs can deposit in the respiratory tract mainly by diffusion, which increases with decreasing air velocity. Model calculation using the Multiple Path Particle Dosimetry (MPPD) model suggests that both tracheobronchial and alveolar regions would receive UFPs (1–100 nm) on the epithelial surface (Braakhuis et al., 2014). Human bronchial and alveolar epithelial cells were consequently the preferred options for toxicity testing of UFPs. However, there are at present only a few human lung cell models available that are resistant to being cultured at ALI, as well as have a good performance on biological barrier (i.e. well-formed tight junctions). The careful selection of the appropriate cell lines was consequently required before starting an exposure.

The aim of this study is to investigate the toxicity of UFPs from aviation and road traffic emissions. We collected UFPs from airport and non-airport emissions (mostly impacted by road traffic) around AMS, as well as UFPs directly from an aircraft turbine engine. An optimized human bronchial epithelial Calu-3 cell model was used in combination with the ALI cloud system to test the toxicity of UFPs samples at 5 exposure doses. The adverse effects as tested by cell viability, lactate dehydrogenase (LDH) release and pro-inflammatory responses were measured at 24 h post exposure and evaluated by the benchmark dose (BMD) analysis.

## 2. Materials and methods

### 2.1. Collection of UFPs samples

#### 2.1.1. Airport and Non-Airport UFPs samples

UFPs from aviation is usually mixed with that of road traffic in airport surroundings, making it difficult to separate the two sources into specific UFPs fractions. To solve this problem, we positioned a UFP sampler at a location (52°19'15.2"N 4°47'07.5"E) between the AMS and two major motorways (A4 and A9), and very close to two major runways within no other major sources in between the sampler and aircrafts (Fig. 1). Fig. 1 illustrated the location of the sampling site, which is as same as the sampling site described in Lammers et al. (2020). Additionally, we took the advantage of the change of wind directions,

allowing sampling UFPs on separate filters at times downwind of airport runways or the major motorways. Samples collected under southern and western wind from direction of the airport were labeled as "Airport" UFPs sample, whereas if the wind was blowing from the direction of the motorways (eastern and northern wind) the samples were labeled as road traffic dominated UFPs (Non-Airport UFPs).

Airport and Non-Airport UFPs samples were collected in 2018, the detailed collecting time can be found in Table 1. Two modified high-volume cascade impactors (HVICI) were used to collect UFPs samples from airport and non-airport emissions respectively using only the final stage with a mass median aerodynamic diameter (MMAD) of less than 0.18  $\mu\text{m}$  as previously described (Demokritou et al., 2002). The decision which HVICI was turned on was made after checking the wind direction. To obtain sufficient UFPs on filters, the sampling time for each filter was for several days, from 9 a.m. to 4 p.m. per day. All filters were weighed by an analytical balance before and after collection (after overnight stabilization at 40–60% humidity and 20 °C) and then stored at –20 °C in the dark.

#### 2.1.2. UFPs samples for turbine and diesel engines

UFPs were also collected directly from the exhaust of a turbine engine (Pratt & Whitney F100) when running at low thrust (ground-idle or taxi operation, Turbine 1) and at full thrust (Turbine 2) using a HVICI. In addition, a standard reference diesel particulate matter (NIST® SRM® 2975) for diesel engine exhaust emissions was purchased (Sigma Aldrich, the Netherlands). Although the NIST diesel sample cannot be used for the direct comparison of the toxicity with the other UFPs samples because of different collection methods, this diesel sample can be used as a benchmark material to assess whether the used biological measurement works and to allow comparison with past and future study findings.

### 2.2. Preparation of particle suspension and characterization

Filters containing UFPs were extracted with methanol by sonication according to the earlier protocol (Gerlofs-Nijland et al., 2013). The extraction procedure was repeated three times. The combined extract from three times was collected in a glass bottle and concentrated using a rotary evaporator (IKA® RV10, Germany) to almost dry matter. 1 mL of methanol was then added to rinse the bottle by a ultrasonic treatment. The remaining suspension was collected into a pre-weighed glass vial, subsequently evaporated overnight at 25 °C, followed by acclimatization (40–60% humidity at 20 °C) for 24 h. The glass vial with residue was then weighed. A clean Teflon TE38 filter was also extracted using the same protocol and included as a negative control. All extracted UFPs samples were stored at –20 °C.

Immediately prior to exposure, the extracted UFPs as well as NIST diesel particles were suspended by ultrasonic treatment in 1 mL of Milli-Q water with 0.01% NaCl solution (for nebulization in cloud system). The particle size distribution of each suspension was measured by a tracing analysis of the Brownian motion with a laser illuminated microscope (LM20, NanoSight Ltd., UK).

### 2.3. ALI culture and TEER measurement

Human bronchial epithelium Calu-3 cell line purchased from the American Tissue Culture Collection (ATCC, Rockville, US) was used for in vitro exposure. Calu-3 cell line was cultured with minimal essential medium (MEM) + GlutaMAX, supplemented with 10% fetal bovine serum (FBS), 1% non-essential amino acid (NEAA) solution and 1% penicillin/streptomycin in an incubator with 5% CO<sub>2</sub> at 37 °C. Upon reaching about 80% confluence, Calu-3 cells were enzymatically detached from the culture flask with 0.05% trypsin-EDTA. 0.5 mL cells suspension with a density of  $2.5 \times 10^5$  cells/mL was seeded into the apical side of sterile 12 mm insert (3.0  $\mu\text{m}$  pore size, 1.12 cm<sup>2</sup> polyester membrane, Costar, Germany) placed in a 12-well plate. 1.5 mL culture



Fig. 1. Location of the sampling site (x) near Amsterdam Airport Schiphol (AMS), same as the sampling site described in Lammers et al. (2020), north-eastern of airport runways and southwestern of two major motorways (A4 and A9).

**Table 1**  
Description and characteristics of particle samples.

Particle samples	Collection period (2018)	Dominating source of emission	Mean size (nm) <sup>1</sup>	Size peaks (nm) <sup>2</sup>
Diesel	N/A	NIST Diesel (reference sample)	177 ± 91	27, 42, 188
Turbine 1	26 April	F100 (low thrust)	204 ± 158	42, 103, 223
Turbine 2	26 April	F100 (full thrust)	70 ± 75	17, 24, 32
Non-airport 1	23, 24 May; 8 June	road traffic contribution	51 ± 64	13, 9, 21
Non-airport 2	12, 13 June; 4–6, 9, 12, 20 July	Road traffic contribution	45 ± 40	29
Non-airport 3	16 October	Road traffic contribution	45 ± 43	30
Airport 1	14, 15 June; 17, 18, 24 July	Aviation contribution	97 ± 102	31, 77
Airport 2	31 July; 8, 15, 22, 29 August; 10, 26 September	Aviation contribution	47 ± 36	32

N/A = not applicable.

<sup>1</sup> . This is the mean size of the particles in suspension and the size can deviate from particle size in the outside air.

<sup>2</sup> . These are the major peaks in the size distribution.

medium was added to the basolateral side of insert for nutrient supply. Cells in insert were cultured under submerged condition for 7 days to achieve confluence. Apical medium was then removed, Calu-3 cells were cultured for an additional 7 days at ALI. Culture medium (only basolateral medium during ALI culture) was refreshed every 2–3 days. All culture medium and supplements were purchased from Life Technologies (Thermo Fisher Scientific Inc., the Netherlands).

As an important indicator of barrier function, transepithelial electrical resistance (TEER) of Calu-3 cells was measured by the Evom2 Voltohmmeter with a 4 mm chopstick electrodes (World Precision Instruments Inc., FL, USA). To measure TEER under ALI condition, 0.5 mL medium was added into the apical side of the insert. All TEER values were corrected for the resistance of cell-free inserts ( $\approx 130 \Omega$ ) and insert surface area ( $1.12 \text{ cm}^2$ ).

#### 2.4. UFPs exposure in cloud exposure system

The VITROCELL® cloud exposure system (Vitrocell, Waldkirch, Germany) was used for ALI in vitro exposure at 37 °C. The system contains 12 cavities for 12 mm inserts including 3 cavities for exposure control inserts, 1 for determining the deposited mass of particles in an insert via a microbalance, and the rest for ALI exposure (Fig. 2A, Lenz et al., 2014). To achieve the ALI exposure to particles, this system uses a single nebulization to produce a dense cloud of droplets with particles in the chamber. The ultrasonic nebulization of the particle suspensions results in 4.0–6.0  $\mu\text{m}$  droplets that are much larger than the size distribution of used particle samples. As such, we do not expect that the nebulization has an impact on the aggregation of the particles. Therefore the particle size distribution of UFPs samples in suspension would be less affected due to the nebulization. Cells were then exposed to the particles by sedimentation of the droplets. Prior to the in vitro exposure, the fluorescein sodium salt (Sigma, the Netherlands) and a reference UFPs sample (DQ12 quartz, IOM, Edinburg) were sprayed via nebulizer respectively to assess the deposition of particles on the

membrane of inserts at exposure positions. The detailed protocol can be found in the supplementary information.

Since pilot in vitro studies already indicated that the effect level was higher than  $0.05 \mu\text{g}/\text{cm}^2$  on the Calu-3 cell model, we designed the exposure procedure by successively nebulizing 100–400  $\mu\text{L}$  of prepared suspension ( $1000 \mu\text{g}/\text{mL}$ ) in the chamber to aim at the doses of UFPs approximately ranging from 0.1 to  $1.5 \mu\text{g}/\text{cm}^2$ . The experiment of each sample includes the following 3 steps: First, 3 inserts for exposure controls were exposed with the suspension of a blank filter extraction or re-suspension solution without particles; Second, 4 exposed doses tested in succession for each UFPs sample, with 2 inserts for each dose (duplicate measurement); Finally, 4 inserts that were not exposed in the cloud system but, with the exception of exposure, treated in the same way including 3 for incubator controls and 1 for measuring the total amount of LDH in cells (see 2.6). The mass of deposited particles via a microbalance was recorded after exposure to the particle aerosol. The actual applied doses in this study vary between the different samples due to the instrumental uncertainty. Overall, most UFPs samples reach the aimed dose range with the exception of Airport 1 sample, in which the highest dose ( $0.96 \mu\text{g}/\text{cm}^2$ ) is much lower compared to the highest dose of the other samples. After exposure, all inserts were transferred to a new 12-wells plates with 1.5 mL fresh culture medium on the basolateral side and cultured in an incubator for 24 h.

#### 2.5. Cell viability

Cell viability was measured by the MTS assay (Promega, Fitchburg, Wisconsin, USA) as previously described (He et al., 2018). Briefly, Calu-3 cells on the membrane after 24 h exposure were washed with culture medium, apical and basolateral medium was collected and stored at 4 °C or  $-20 \text{ }^\circ\text{C}$  for analysis. Subsequently, cells were incubated with 500  $\mu\text{L}$  fresh MTS solution (medium: MTS reagent = 9: 1). After 30 min incubation, 100  $\mu\text{L}$  MTS solution was transferred into 96-well flat bottom plates (Thermo Fisher Scientific Inc., the Netherlands) for

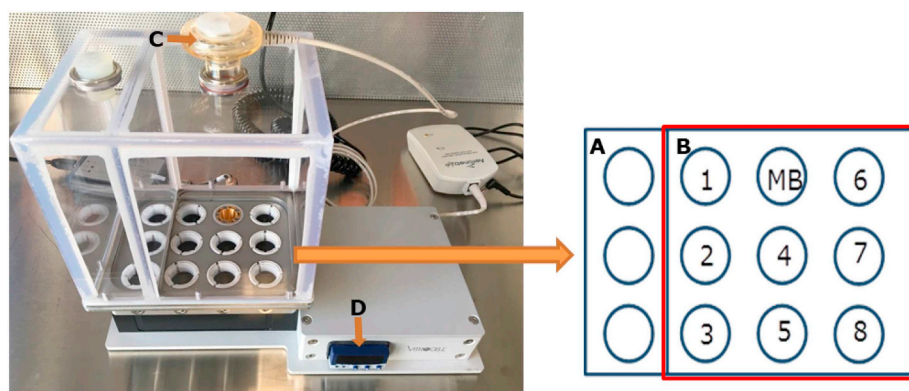


**Fig. 2.** Air-liquid interface (ALI) cloud exposure system. A: Chamber for exposure controls; B: Chamber for UFPs exposure, number 1–8 represents each exposure position, MB represents a microbalance; C: Aerosol nebulizer (pore size: 4.0–6.0  $\mu\text{m}$ ); D: Temperature controller. More detailed information can be found via the following link: <https://www.vitrocell.com/inhalation-toxicology/exposure-systems/vitrocell-cloud-system>

absorption measurement. MTS solution was used as a blank control. The viability of exposed cells was corrected for incubator controls.

## 2.6. LDH leakage

The leakage of total lactate dehydrogenase (LDH) in culture medium was measured with the LDH cytotoxicity detection kit (Roche Diagnostics GmbH, Mannheim, Germany). 100  $\mu$ L of collected apical or basolateral medium and reaction reagent were successively added into 96-well flat bottom plates and incubated in dark at room temperature for 20 min. After adding 50  $\mu$ L stop solution (HCl, 1.0 M, Sigma, the Netherlands), absorbance was measured at 490 nm (with background subtraction at 650 nm). Culture medium was tested as a blank control. All LDH values are corrected for the total amount of LDH in cells. To measure the total amount of LDH, cells in an insert (incubator control) were lysed with 2% triton X-100 (Thermo Fisher Scientific Inc., the Netherlands) for 5 min.

## 2.7. Release of pro-inflammatory mediators

To investigate effects of particles on pro-inflammatory responses, the production of pro-inflammatory mediators (IL-6 and IL-8) in basolateral medium was measured using the enzyme-linked immunosorbent assay (ELISA) kit (eBioscience, San Diego, USA). As a positive control substance, lipopolysaccharide (LPS) was sprayed to the apical side of Calu-3 model for inducing pro-inflammatory responses. The detailed exposure protocol can be found in the supplementary information.

## 2.8. Statistical analysis

Applying the adverse responses at 5 dose groups, the benchmark dose (BMD) analysis (EFSA, 2009) was performed with PROAST (version 65.2 [www.rivm.nl/proast](http://www.rivm.nl/proast)) to create a dose-response relationship for each UFPs sample. This analysis has the advantage that it estimates the BMD with a confidence interval, increasing the reliability of outcomes and allowing to compare the toxicity of UFPs samples. The detailed description of BMD analysis can be found in our earlier study (Gosens et al., 2016). The analysis was performed at a defined effect size (benchmark response (BMR)). For the release of LDH and inflammatory mediators (IL-6 and IL-8), a BMR of 10% change compared to the incubator control level was chosen according to the EFSA (2009). When applying this statistical analysis at the predefined BMR, several dose-response models were fitted to results and the optimal model would be turned out after modeling. The Hill model was used in the present study and lower 5% and upper 95% confidence limits (one sided, BMDL and BMDU, respectively) of the corresponding BMD as well as mean BMD were derived with the Hill model. The 90% BMD confidence interval (BMD<sub>c.i.</sub>) including BMDL, BMDU, and average BMD values was presented per effect marker that represented the degree of toxicity. The narrower the BMD<sub>c.i.</sub> is, the more certain this dose interval can lead to the predefined effect. The BMD<sub>c.i.</sub> was also used for potency comparison between UFPs samples (EFSA, 2009). The more overlapping between BMD<sub>c.i.</sub> implies less difference in the potency of UFPs samples. If there is no 10% change or no BMDU determined at applied doses, the UFPs sample was not included in the comparison.

## 3. Results

### 3.1. UFPs samples description

The description and size distributions of the particle samples are presented in Table 1. It should be noticed that this is the size distribution of the particles in suspension that can deviate from particle size in the outside air. The mean size of the particles samples in suspension falls within the ultrafine range as defined in this study (< 180 nm) with the exception of Turbine 1 sample (204 nm). The

mean size of each Non-Airport sample is approximately 50 nm, which is similar to the mean size of the Airport 2 sample. In comparison, the mean size of the Airport 1 sample (97 nm) is twice as large.

### 3.2. Particles deposition in ALI cloud system and TEER of Calu-3 cells

A fluorescein sodium salt was used to assess the deposition of parties in ALI cloud system. Although it is a soluble chemical, as we have generated an aerosol that either included the fluorescein or the collected/purchased particles, we have used this to demonstrate if the droplets themselves were uniformly distributed. On the basis of the fluorescence images, distributions of the fluorescein salt were homogeneous on the membrane of each insert in exposure position. The fluorescence intensity was similar between exposure inserts as well (Fig. S1). It indicates the fluorescein deposition was uniform within each exposure well and constant across the different wells. Moreover, after nebulization with the cloud system the deposition of DQ12 quartz ( $\approx$  150 nm in suspension) on membranes of inserts, as a reference, was also analyzed via a TEM. As shown in Fig. S2, most of particles were evenly deposited on the membrane, while several particles cluster appeared, probably because of the agglomeration and aggregation of particles in the suspension.

To check that Calu-3 cells do form the tight barrier after 14 days (7 days at submerge and 7 days at ALI) culture, TEER of Calu-3 cells was measured before starting the exposure. As shown in Fig. 3A, Calu-3 cells used for in vitro exposure can express high TEER ( $> 800 \Omega \times \text{cm}^2$ ) levels, indicating well-formed tight junction and suitability for particles exposure via ALI cloud system. TEER of Calu-3 cells was also measured after 24 h exposure to Airport and Non-Airport UFPs (Fig. 3B). All TEER values at each exposed dose showed a slight drop to around  $600 \Omega \times \text{cm}^2$ , indicating the barrier function in Calu-3 cells still remained upon exposure.

### 3.3. Cell viability and cytotoxicity

After 24 h exposure, cell viabilities are higher than 80% for all particles samples at the exposed doses (Fig. 4). LDH release in the medium (apical + basolateral) was also measured (Fig. 5) as a marker for cell membrane damage and cytotoxicity. In general, an increased LDH release is only observed at the highest exposed dose around  $1.5 \mu\text{g}/\text{cm}^2$  for most of UFPs samples. For the reference sample (NIST diesel), a clear dose-response relationship can be observed at exposure levels ranging from 0 to  $3.6 \mu\text{g}/\text{cm}^2$ .

A BMD analysis was performed to rank the UFPs samples based on the degree of cytotoxicity, BMD values inducing a 10% increase in LDH level were obtained, including the mean BMD, the lower (BMDL) and upper (BMDU) limits of the BMD<sub>c.i.</sub> (Fig. 6 and Table 3). The BMDU for Airport 1 sample could not be determined and Non-Airport 1 sample dose not induce the BMR at exposed doses. It indicates the low cytotoxicity of Airport 1 and Non-Airport 1 samples, which are not included in the comparison. BMDs for the other Airport and Non-Airport samples as well as turbine and diesel samples can be determined, however, no distinctions in LDH levels could be made because of the substantial overlap between their BMD<sub>c.i.</sub> (NIST diesel sample is not used for the comparison because of different collection methods).

### 3.4. IL-6 and IL-8 production

The production of pro-inflammatory mediators (IL-6 and IL-8) in Calu-3 cells was measured after 24 h exposure (Table 2). Exposure to UFPs collected from airport and non-airport emissions as well as from a turbine engine at low thrust (Turbine 1) can promote the production of IL-6 and IL-8 mainly at the highest applied dose. When using LPS as a positive control substance to induce pro-inflammatory response (IL-8), Calu-3 cells do show an increased IL-8 secretion ( $> 2.5$  folds), which gives confidence that Calu-3 model is capable of detecting pro-



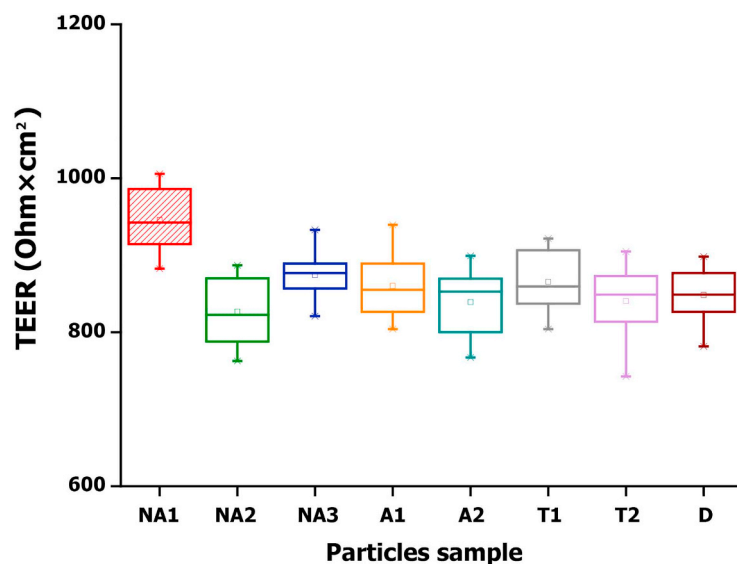


Fig. 3A. TEER of Calu-3 cells at ALI before being used for in vitro exposure to UFPs samples. NA and A represent Non-Airport and Airport samples, T represents Turbine sample, D represents Diesel sample. Calu-3 cells were at submerged culture for 7 days, followed by ALI culture for 7 days.

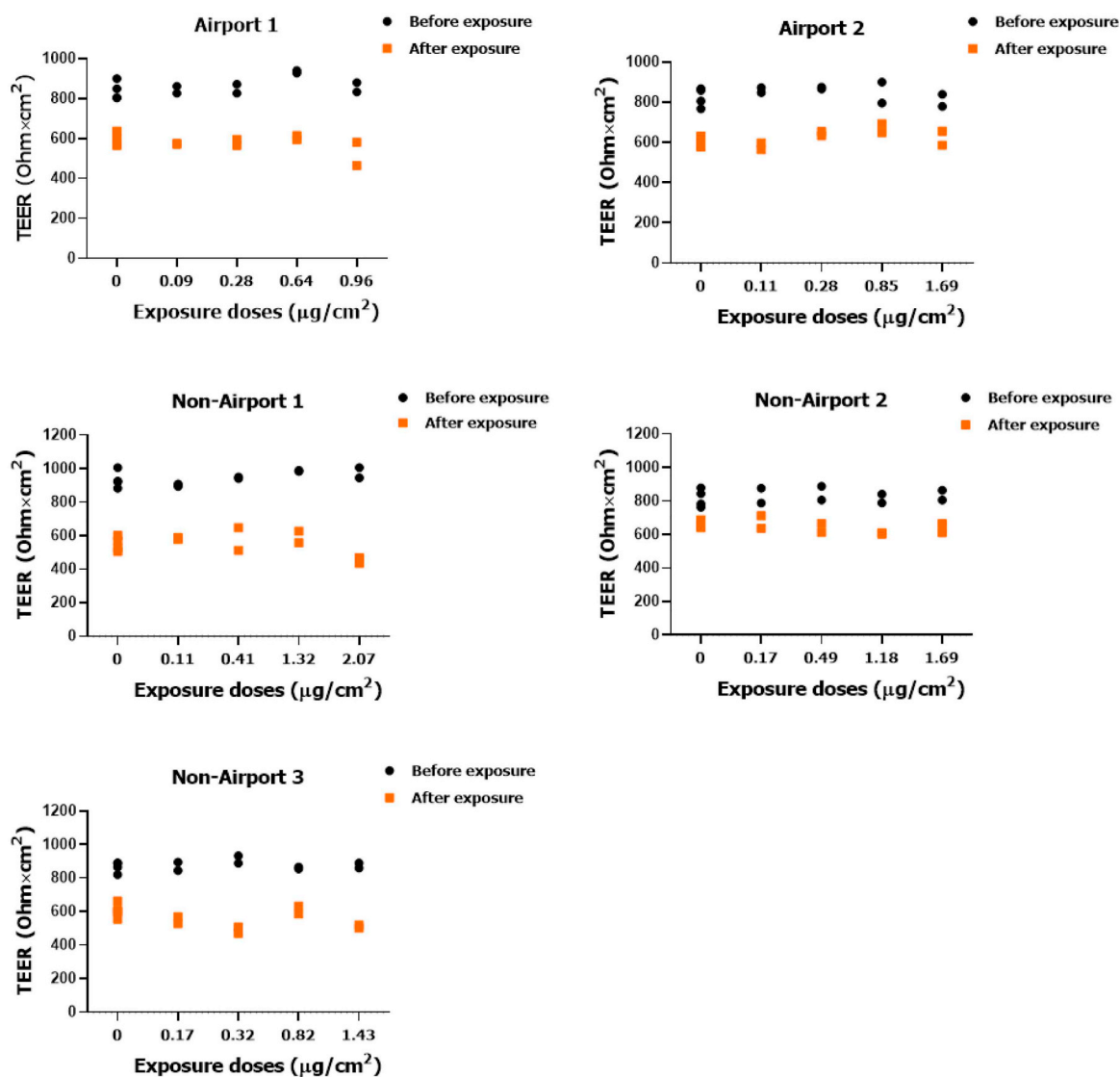
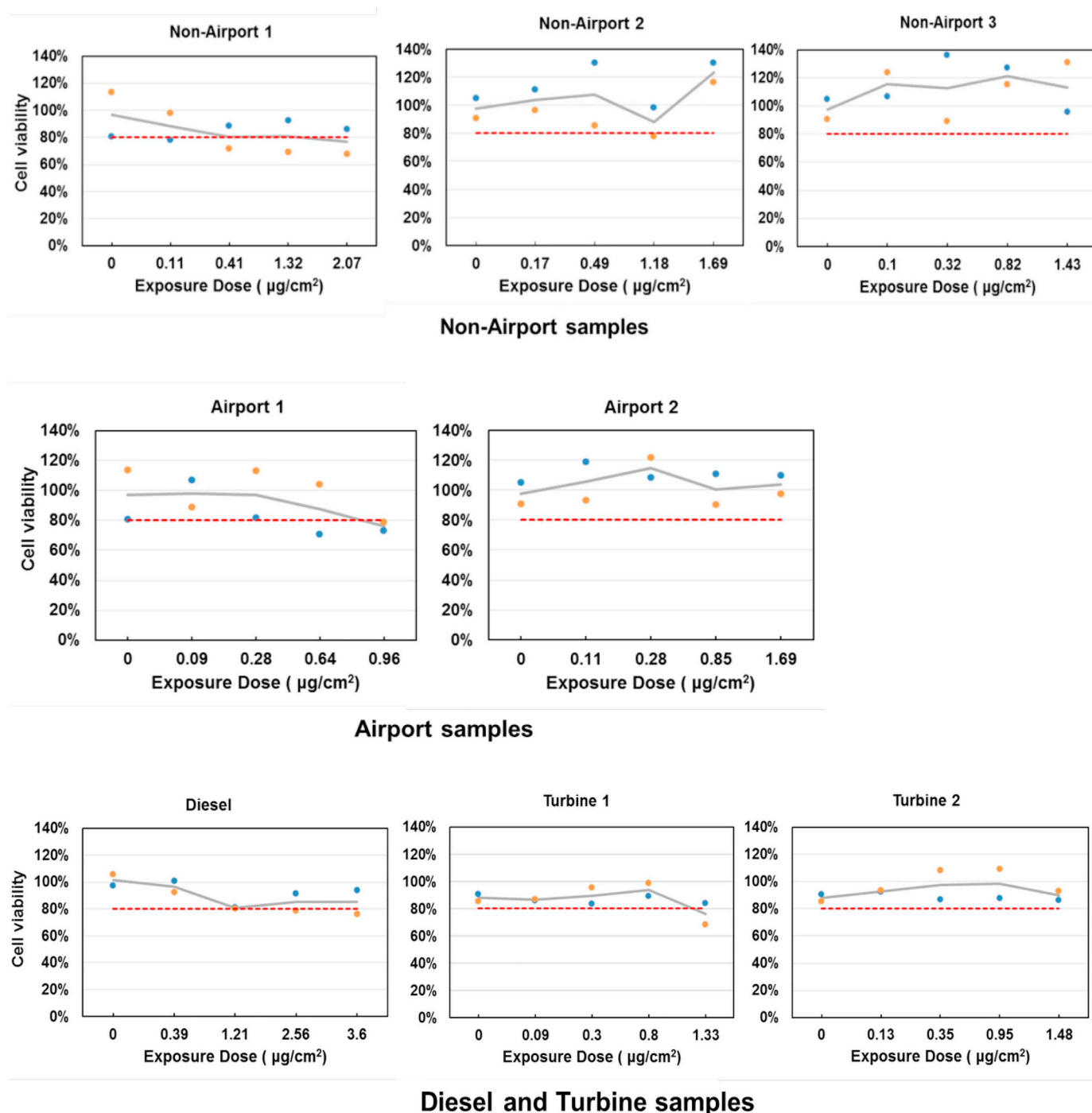


Fig. 3B. TEER changes of Calu-3 cells after 24 h exposure to Airport and Non-Airport UFPs at ALI.



**Fig. 4.** Cell viability tested by MTS after exposing to UFPs samples for 24 h. The dots represent viability values from the duplicate measurement at applied doses and the trend line was made by average cell viability values at each dose. The dotted line is 80% viability, above which indicates few effects on cell death.

inflammatory responses (Fig. S3).

According to the outcomes of the performed “BMD analysis” (Fig. 7 and Table 3), a 10% BMR could be identified for all particle samples with the exception of Turbine 2 and NIST diesel, indicating few effects on IL-6 and IL-8 production for Turbine 2 and diesel samples at used doses. However, due to the substantial overlapped BMDc.i. between Airport and Non-Airport UFPs samples, no distinctions in cytokines IL-6 and IL-8 levels could be made.

#### 4. Discussion

Our findings show that cell damage and the secretion of pro-

inflammatory mediators can occur in a Calu-3 model after exposure to UFPs from airport or a non-airport emission as well as from an aircraft turbine engine. There are no indications that the health effects of airport emission are substantially different from those caused by road traffic emissions applying similar exposure doses (on a mass basis).

The exposed doses (0.09 to 2.07  $\mu\text{g}/\text{cm}^2$ ) of particles in this study are substantially lower than those have been previously reported in other in vitro studies. For example, the research on Los Angeles International Airport (LAX), in which the toxicity of  $\text{PM} < 0.25 \mu\text{m}$  collected from aviation activities and urban traffic area was compared, assumed a dosage of 3.13  $\mu\text{g}/\text{cm}^2$  (He et al., 2018). In the RAPTES study (Steenhof et al., 2011), increasing doses from 3.68 to 58.8  $\mu\text{g}/\text{cm}^2$  were

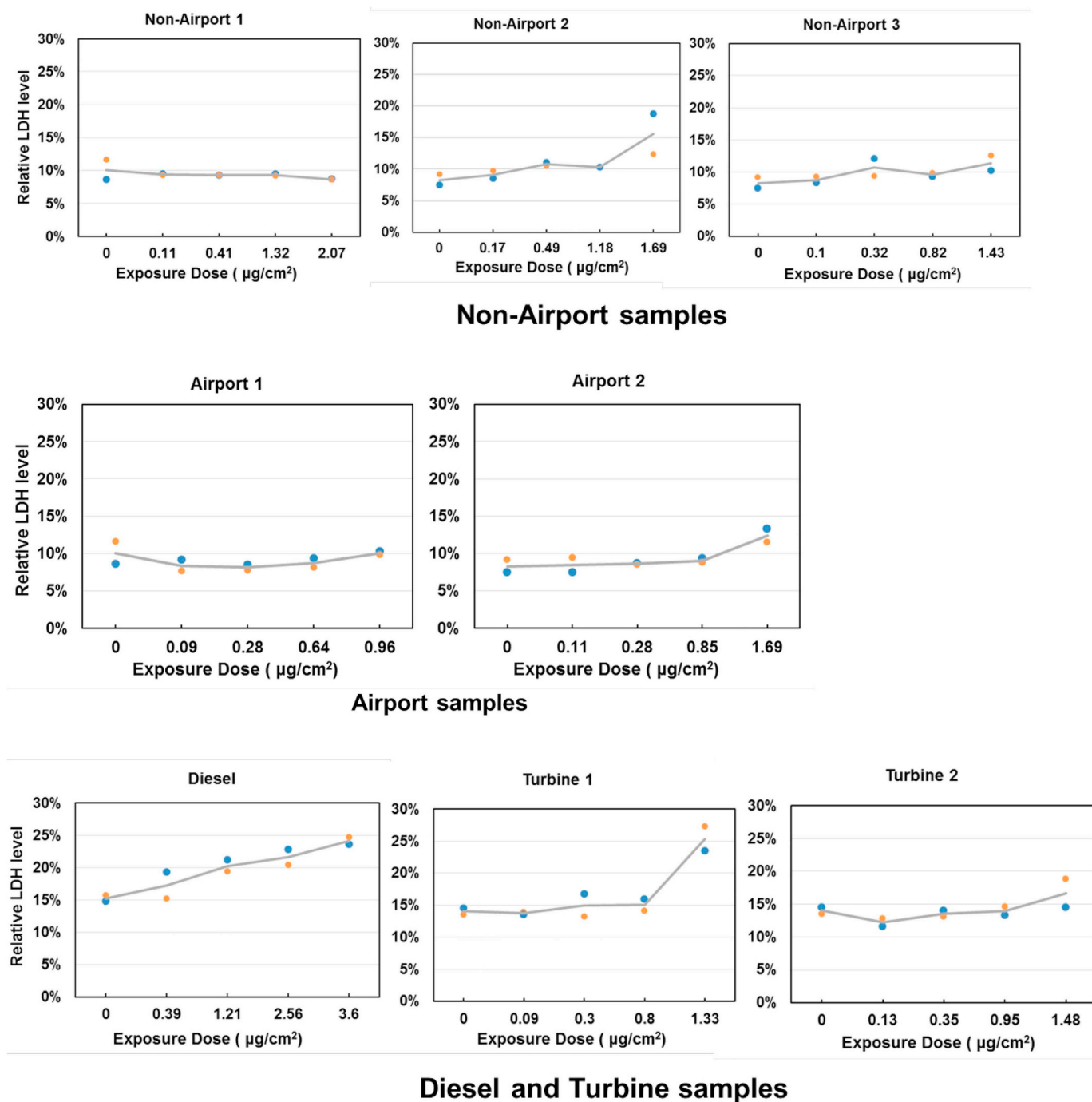
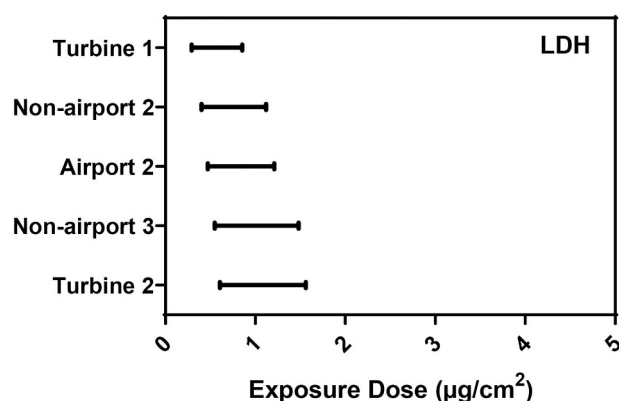


Fig. 5. Relative LDH release of Calu-3 cells after exposing to UFPs samples for 24 h. The dots represent LDH levels from the duplicate measurement at applied doses and the trend line was made by the average LDH levels at each dose.

used to compare the in vitro toxicity of PM samples with three size fractions and from different sources in the Netherlands. Comparable doses of particles used in our study were also used in a recent in vitro study, in which human bronchial epithelial (BEAS-2B) cells were directly exposed to diluted emissions from a turbine engine under stationary condition at very low doses (2.1–6.9 ng/cm<sup>2</sup>) and at doses of 0.3–0.4 µg/cm<sup>2</sup> with the engine speed corresponding to ascending airplanes (Jonsdottir et al., 2019). Comparing the exposure levels used in those in vitro studies to levels people are actually exposed to in the environment, including airport surroundings, is difficult. Especially for UFPs when exposure doses related to mass concentrations are used, while for ultrafine particles particle size and particle number

concentrations may be more relevant.

To our knowledge, this is the first ALI exposure to air pollution UFPs done with Calu-3 model. For the reference diesel sample a clear increase in LDH release was seen with the exposure doses increase, however, production of IL-6 and IL-8 induced at each dose were at comparable level to the exposure control (0 µg/cm<sup>2</sup>). This low production of pro-inflammatory cytokines was also observed in another bronchial epithelial (BEAS-2B) cells line after exposure to diesel particles (SRM 2975) at doses ranging from 1.0 µg/cm<sup>2</sup> to 110 µg/cm<sup>2</sup> (Chaudhuri et al., 2010). A possible explanation for the limited induction of pro-inflammatory response is that the large size distribution of diesel particles ( $\approx 177 \pm 91$  nm) might lead to the less cellular



**Fig. 6.** Summary of derived BMDs and confidence interval in LDH levels for which a dose–response was found within applied doses. The BMDU for Airport 1 sample could not be determined and Non-Airport 1 sample did not induce the BMR. Both samples were not included in the comparison.

**Table 2**

The concentration of pro-inflammatory mediators (IL-6 and IL-8) in basolateral side medium after exposing to UFPs samples at 5 doses for 24 h.

Particle samples	Exposure Dose ( $\mu\text{g}/\text{cm}^2$ )	Concentration ( $\text{pg}/\text{mL}$ )	
		IL-6	IL-8
Diesel	0	2891	15,926
	0.39	2569	14,151
	1.21	2910	16,027
	2.56	2816	15,509
	3.60	3081	16,971
Turbine 1	0	2517	13,866
	0.09	2640	14,541
	0.30	3003	16,543
	0.80	2726	15,016
	1.33	3045	16,770
Turbine 2	0	2517	13,866
	0.13	1821	11,529
	0.35	2058	13,031
	0.95	2117	13,402
	1.48	1977	12,515
Non-airport 1	0	1108	6663
	0.11	999	6321
	0.41	957	6056
	1.32	1053	6665
	2.07	1350	8549
Non-airport 2	0	1489	10,687
	0.17	1333	9563
	0.49	1615	11,585
	1.18	1600	11,476
	1.69	1866	13,389
Non-airport 3	0	1489	10,687
	0.10	1522	10,923
	0.32	1788	12,825
	0.82	1737	12,464
	1.43	1928	13,830
Airport 1	0	1108	6663
	0.09	909	5753
	0.28	955	6045
	0.64	1166	7379
	0.96	1496	9469
Airport 2	0	1489	10,687
	0.11	1562	11,208
	0.28	1599	11,474
	0.85	1965	14,096
	1.69	2024	14,519

internalization of particles, thus limiting the release of pro-inflammatory cytokines in Calu-3 cells (Hussain et al., 2009; He et al., 2018). In line with the growing awareness that cellular adverse effects including the inflammation can still be induced at high cell viability (Bitterle et al., 2006; He et al., 2018), up-regulation of pro-

inflammatory mediators (10% increase of IL-6 and IL-8 secretion) was observed in Calu-3 cells after Airport and Non-Airport UFPs exposure at levels ranging from 0.35 to 1.0  $\mu\text{g}/\text{cm}^2$  (Table 3). The effect doses of UFPs on Calu-3 cells that cause the pro-inflammatory responses under ALI exposure are substantially lower in comparison with those on Calu-3 cells using submerged exposure (Mura et al., 2011; Puisney et al., 2018). For example, Puisney et al. (2018) reported only limited up-regulation of inflammatory marker (IL-6) in Calu-3 cells after submerged exposure to the nano-sized particles at dose of 1.0–10  $\mu\text{g}/\text{cm}^2$ . The exposure method may be a critical factor influencing the effect dose. Compared to the traditional submerged exposure via medium, ALI exposure reflects more relevant and realistic human inhalation exposure, allowing particles to be deposited at the epithelial cell surface instead of agglomeration and diffusion in the medium (Limbach et al., 2005), consequently resulting in the lower effect doses of UFPs under ALI exposure. A recent review about in vitro exposures also concluded that in relation to the production of the inflammatory marker (IL-8) after particles exposure, the deposited dose recorded at ALI exposure is more informative than the administered dose used for submerged exposure (Secondo et al., 2017).

Besides the exposure method, effect doses can also be influenced by cell types used in ALI exposure. Jonsdottir et al. (2019) performed an in vitro exposure at ALI with similar design, which showed the over-production of inflammatory mediators (IL-6 and IL-8) in human bronchial epithelial (BEAS-2B) cells after exposing to diluted emissions from a stationary engine at very low doses (2.1–6.9  $\text{ng}/\text{cm}^2$ ). These low effect doses may indicate the higher sensitivity in BEAS-2B cells than that in Calu-3 cells when exposed to UFPs under ALI condition. The high resistance in Calu-3 cells at ALI might be an explanation. ALI condition promotes the differentiation of Calu-3 cells in producing the thick mucus and forming the tight junction, which are the functional characteristics in lungs (Grainger et al., 2006; Vlasaliu et al., 2011). The mucociliary clearance and well-formed tight junction can therefore provide much more resistance to particles exposure in Calu-3 cells compared to other in vitro models (e.g. BEAS-2B and A549 cells) with the weak cellular clearance and tight junction formation at ALI (Bitterle et al., 2006; Heijink et al., 2010). Such high resistance in Calu-3 cells at ALI was also reported in Banga et al. (2012), showing that no changes were detected in levels of some cytokines including IL-8 in Calu-3 cells (ALI culture for 14 days) after exposing to nanoparticles (< 100 nm) at 4  $\mu\text{g}/\text{cm}^2$  and 4  $\text{ng}/\text{cm}^2$ . However, that lack of macrophages, which is a limitation of the current epithelial Calu-3 model, might be another explanation of lower sensitivity of this cell type for cytokine production. Possibly, macrophages can produce pro-inflammatory mediators after the uptake of UFPs that subsequently may affect Calu-3 cells, promoting cellular responses to UFPs (Hu and Christman, 2019).

When starting a risk assessment of exposure to UFPs, BMDs for various cellular responses can be used to identify the degree of toxicity (EFSA, 2009). Substantial overlap between the BMD<sub>c.i.</sub> of UFPs from airport and non-airport emissions was shown in LDH, IL-6 and IL-8 levels, which indicates the comparable ability of these UFPs samples to induce the cytotoxicity and pro-inflammatory responses in Calu-3 cells. An explanation for their similar toxicity is the mild effects on the cytotoxicity and inflammation, which might be due to the low deposited dose. With the mild effects, the range of BMD<sub>c.i.</sub> is wide, which makes the BMD<sub>c.i.</sub> of UFPs samples difficult to distinguish. The insignificant difference on size distribution between Airport and Non-Airport UFPs might be another explanation. A large amount of research has reported differences in size can lead to different toxicity of particles. Particles in smaller size can absorb more organic and inorganic substances and deposit on the respiratory tract with higher efficiency, which increase their toxicity per unit of inhaled mass (Terzano et al., 2010; Li et al., 2003; Schwarze et al., 2006). Unlike previous findings that the particle size in airport emission was clearly smaller than that in road traffic emission (Keuken et al., 2015; Shirmohammadi et al., 2017), size distributions of airport and road traffic UFPs samples are similar in the



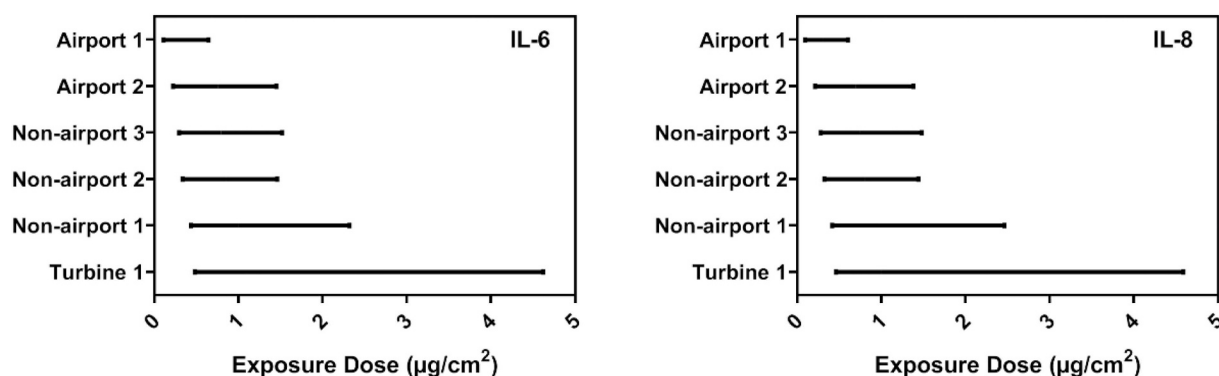


Fig. 7. Summary of derived BMDs and confidence interval in IL-6 and IL-8 levels for which a dose–response was found within applied doses. Turbine 2 sample did not induce a BMR and was therefore not included in the comparison.

Table 3

Summary of derived BMDs in LDH, IL-6 and IL-8 levels including the mean BMD, lower (BMDL) and upper (BMDU) limits of the confidence interval inducing a 10% BMR.

BMR:10%	BMDs ( $\mu\text{g}/\text{cm}^2$ )								
	LDH			IL-6			IL-8		
	Mean	BMDL	BMDU	Mean	BMDL	BMDU	Mean	BMDL	BMDU
Turbine 1	0.58	0.29	0.84	1.1	0.48	4.62	1.0	0.46	4.59
Turbine 2	0.98	0.62	1.56	–	–	–	–	–	–
Non-airport 1	–	–	–	1.0	0.43	2.32	0.98	0.42	2.46
Non-airport 2	0.78	0.40	1.12	0.86	0.34	1.46	0.81	0.32	1.44
Non-airport 3	0.94	0.55	1.48	0.79	0.29	1.52	0.75	0.28	1.45
Airport 1	0.87	0.55	–	0.35	0.11	0.66	0.31	0.09	0.60
Airport 2	0.87	0.47	1.21	0.76	0.22	1.45	0.7	0.21	1.38
Diesel <sup>1</sup>	1.9	1.01	2.69	3.5	1.7	–	3.5	1.65	–

“–”: could not be determined.

<sup>1</sup> . NIST diesel sample is not used for the direct comparison of the toxicity to the other UFPs samples because of different collection methods

present study with the exception of Airport 1 sample which is even twice as large as the mean size. This indicated that size distribution in UFPs suspension may differ from size distribution of UFPs in ambient air, since the smaller particles can easily clump together and form larger particles during collecting and extracting the UFPs in/from the filter (Yu et al., 1997). To overcome this limitation, the combination of particles sampling system and ALI exposure system can be implemented to provide the real-time UFPs exposure. The optimization of the ALI exposure system is currently ongoing.

## 5. Conclusion

UFPs from airport, non-airport (road traffic) origin as well as from a turbine engine can induce the cell damage and release of pro-inflammatory markers. No substantial differences are identified among UFPs samples in their toxic potency at the applied doses, suggesting that UFPs from airport and road traffic in airport surroundings may have similar adverse effects on public health.

## Declaration of Competing Interest

The authors declare that they have no known competing financial interests or personal relationships that could have appeared to influence the work reported in this paper.

## Acknowledgements

This research has been commissioned by the Dutch Ministry of Infrastructure and Water management for the research program M240045 “Gezondheidsrisico's ultrafijn stof rond Schiphol”. We thank

Eric Gremmer and Ilse Gosens from the National Institute for Public Health and the Environment (RIVM) for their valuable assistance with the in vitro measurements, BMD analysis. We thank Remco Westerink from the Institute for Risk Assessment Sciences (IRAS), Utrecht University for his insightful comments on the manuscript. We are also grateful to Barbara Drasler and Dimitri Vanhecke from the Adolphe Merkle Institute, University of Fribourg for their kind assistance with the TEM microscopy. The support provided by China Scholarship Council (CSC) during the PhD period of Rui-Wen He in Utrecht University- IRAS is also acknowledged.

## Appendix A. Supplementary data

Supplementary data to this article can be found online at <https://doi.org/10.1016/j.tiv.2020.104950>.

## References

- Antherieu, S., Garat, A., Beauval, N., Soyez, M., Allorge, D., Garcon, G., Lo-Guidice, J.-M., 2017. Comparison of cellular and transcriptomic effects between electronic cigarette vapor and cigarette smoke in human bronchial epithelial cells. *Toxicol. in Vitro* 45, 417–425.
- Banga, A., Witzmann, F.A., Petrache, H.I., Blazer-Yost, B.L., 2012. Functional effects of nanoparticle exposure on Calu-3 airway epithelial cells. *Cell. Physiol. Biochem.* 29, 197–212.
- BéruBé, K., Prytherch, Z., Job, C., Hughes, T., 2010. Human primary bronchial lung cell constructs: the new respiratory models. *Toxicology* 278, 311–318.
- Bitterle, E., Karg, E., Schroepel, A., Kreyling, W., Tippe, A., et al., 2006. Dose-controlled exposure of A549 epithelial cells at the air–liquid interface to airborne ultrafine carbonaceous particles. *Chemosphere* 65, 1784–1790.
- Braakhuis, H.M., Park, M.V., Gosens, I., De Jong, W.H., Cassee, F.R., 2014. Physicochemical characteristics of nanomaterials that affect pulmonary inflammation. *Particle Fibre Toxicol.* 11 (1), 18.
- Chaudhuri, N., Paiva, C., Donaldson, K., Duffin, R., Parker, L.C., Sabroe, I., 2010. Diesel

- exhaust particles override natural injury-limiting pathways in the lung. *Am. J. Phys. Lung Cell. Mol. Phys.* 299 L263-L71.
- Demokritou, P., Kavouras, I., Ferguson, S., Koutrakis, P., 2002. Development of a high volume cascade impactor for toxicological and chemical characterization studies. *Aerosol Sci. Technol.* 36, 925–933.
- EFSA, 2009. Guidance of the scientific committee on use of the benchmark dose approach in risk assessment. *EFSA J.* 7 (6), 1150.
- Fizeşan, I., Cambier, S., Moschini, E., Chary, A., Nelissen, I., Ziebel, J., Audinot, J.-N., Wirtz, T., Kruszewski, M., Pop, A., 2019. In vitro exposure of a 3D-tetraculture representative for the alveolar barrier at the air-liquid interface to silver particles and nanowires. *Particle Fibre Toxicol.* 16, 14.
- Gerlofs-Nijland, M.E., Totlandsdal, A.I., Tzamkiozis, T., Leleman, D.L.C., Samaras, Z., et al., 2013. Cell toxicity and oxidative potential of engine exhaust particles: impact of using particulate filter or biodiesel fuel blend. *Environ. Sci. Technol.* 47, 5931–5938.
- Gosens, I., Cassee, F.R., Zanella, M., Manodori, L., Brunelli, A., et al., 2016. Organ burden and pulmonary toxicity of nano-sized copper (II) oxide particles after short-term inhalation exposure. *Nanotoxicology* 10, 1084–1095.
- Grainger, C.I., Greenwell, L.L., Lockley, D.J., Martin, G.P., Forbes, B., 2006. Culture of Calu-3 cells at the air interface provides a representative model of the airway epithelial barrier. *Pharm. Res.* 23, 1482–1490.
- He, R.-W., Shirmohammadi, F., Gerlofs-Nijland, M.E., Sioutas, C., Cassee, F.R., 2018. Pro-inflammatory responses to PM<sub>0.25</sub> from airport and urban traffic emissions. *Sci. Total Environ.* 640, 997–1003.
- Heijink, I.H., Brandenburg, S.M., Noordhoek, J.A., Postma, D.S., Slebos, D.-J., van Oosterhout, A.J., 2010. Characterisation of cell adhesion in airway epithelial cell types using electric cell-substrate impedance sensing. *Eur. Respir. J.* 35, 894–903.
- Heusinkveld, H.J., Wahle, T., Campbell, A., Westerink, R.H., Tran, L., et al., 2016. Neurodegenerative and neurological disorders by small inhaled particles. *Neurotoxicology* 56, 94–106.
- Hu, G., Christman, J.W., 2019. Alveolar macrophages in lung inflammation and resolution. *Front. Immunol.* 10, 2275.
- Hudda, N., Fruin, S., 2016. International airport impacts to air quality: size and related properties of large increases in ultrafine particle number concentrations. *Environ. Sci. Technol.* 50, 3362–3370.
- Hussain, S., Boland, S., Baeza-Squiban, A., Hamel, R., Thomassen, L.C., Martens, J.A., Billon-Galland, M.A., Fleury-Feith, J., Moisan, F., Pairon, J.-C., 2009. Oxidative stress and proinflammatory effects of carbon black and titanium dioxide nanoparticles: role of particle surface area and internalized amount. *Toxicology* 260, 142–149.
- Jonsdottir, H.R., Delaval, M., Leni, Z., Keller, A., Brem, B.T., et al., 2019. Non-volatile particle emissions from aircraft turbine engines at ground-idle induce oxidative stress in bronchial cells. *Commun. Biol.* 2, 90.
- Keuken, M., Moerman, M., Zandveld, P., Henzing, J., Hoek, G., 2015. Total and size-resolved particle number and black carbon concentrations in urban areas near Schiphol airport (the Netherlands). *Atmos. Environ.* 104, 132–142.
- Kim, H.R., Lee, K., Park, C.W., Song, J.A., Park, Y.J., Chung, K.H., 2016. Polyhexamethylene guanidine phosphate aerosol particles induce pulmonary inflammatory and fibrotic responses. *Arch. Toxicol.* 90, 617–632.
- Lammers, A., Janssen, N.A.H., Boere, A.J.F., Berger, M., Longo, C., Vijverberg, S.J.H., Neerincx, A.H., Maitland - van der Zee, A.H., Cassee, F.R., 2020. Effects of short-term exposures to ultrafine particles near an airport in healthy subjects. *Environ. Int.* 141, 105779.
- Lenz, A.-G., Stoeger, T., Cei, D., Schmidmeir, M., Semren, N., et al., 2014. Efficient bioactive delivery of aerosolized drugs to human pulmonary epithelial cells cultured in air-liquid interface conditions. *Am. J. Respir. Cell Mol. Biol.* 51, 526–535.
- Li, N., Sioutas, C., Cho, A., Schmitz, D., Misra, C., et al., 2003. Ultrafine particulate pollutants induce oxidative stress and mitochondrial damage. *Environ. Health Perspect.* 111, 455.
- Limbach, L.K., Li, Y., Grass, R.N., Brunner, T.J., Hintermann, M.A., et al., 2005. Oxide nanoparticle uptake in human lung fibroblasts: effects of particle size, agglomeration, and diffusion at low concentrations. *Environ. Sci. Technol.* 39, 9370–9376.
- Masiol, M., Harrison, R.M., 2014. Aircraft engine exhaust emissions and other airport-related contributions to ambient air pollution: a review. *Atmos. Environ.* 95, 409–455.
- Miller, M.R., Raftis, J.B., Langrish, J.P., McLean, S.G., Samutrtai, P., et al., 2017. Inhaled nanoparticles accumulate at sites of vascular disease. *ACS Nano* 11, 4542–4552.
- Mühlhopt, S., Dilger, M., Diabaté, S., Schlager, C., Krebs, T., Zimmermann, R., Buters, J., Oeder, S., Wäscher, T., Weiss, C., 2016. Toxicity testing of combustion aerosols at the air-liquid interface with a self-contained and easy-to-use exposure system. *J. Aerosol Sci.* 96, 38–55.
- Mura, S., Hillaireau, H., Nicolas, J., Le Droumaguet, B., Gueutin, C., et al., 2011. Influence of surface charge on the potential toxicity of PLGA nanoparticles towards Calu-3 cells. *Int. J. Nanomedicine* 6, 2591.
- Pirhadi, M., Mousavi, A., Sowlat, M.H., Janssen, N.A., Cassee, F.R., Sioutas, C., 2020. Relative contributions of a major international airport activities and other urban sources to the particle number concentrations (PNCs) at a nearby monitoring site. In: *Environmental Pollution*: 114027.
- Puisney, C., Oikonomou, E.K., Nowak, S., Chevillot, A., Casale, S., et al., 2018. Brake wear (nano) particle characterization and toxicity on airway epithelial cells in vitro. *Environ. Sci.* 5, 1036–1044.
- Ren, J., Cao, X., Liu, J., 2018. Impact of atmospheric particulate matter pollutants to IAQ of airport terminal buildings: a first field study at Tianjin airport, China. *Atmos. Environ.* 179, 222–226.
- Riley, E.A., Gould, T., Hartin, K., Fruin, S.A., Simpson, C.D., et al., 2016. Ultrafine particle size as a tracer for aircraft turbine emissions. *Atmos. Environ.* 139, 20–29.
- Schwarze, P., Øvreivik, J., Låg, M., Refsnes, M., Nafstad, P., et al., 2006. Particulate matter properties and health effects: consistency of epidemiological and toxicological studies. *Hum. Exp. Toxicol.* 25, 559–579.
- Secondo, L.E., Liu, N.J., Lewinski, N.A., 2017. Methodological considerations when conducting in vitro, air-liquid interface exposures to engineered nanoparticle aerosols. *Crit. Rev. Toxicol.* 47, 225–262.
- Shirmohammadi, F., Lovett, C., Sowlat, M., Mousavi, A., Verma, V., et al., 2017. Chemical composition and redox activity of PM<sub>0.25</sub> near Los Angeles international airport and comparisons to an urban traffic site. *Sci. Total Environ.* 610, 1336.
- Stacey, B., 2019. Measurement of ultrafine particles at airports: a review. *Atmos. Environ.* 198, 463–477.
- Steenhof, M., Gosens, I., Strak, M., Godri, K.J., Hoek, G., et al., 2011. In vitro toxicity of particulate matter (PM) collected at different sites in the Netherlands is associated with PM composition, size fraction and oxidative potential-the RPTES project. *Particle Fibre Toxicol.* 8, 26.
- Stone, V., Miller, M.R., Clift, M.J., Elder, A., Mills, N.L., et al., 2017. Nanomaterials versus ambient ultrafine particles: an opportunity to exchange toxicology knowledge. *Environ. Health Perspect.* 125, 106002.
- Terzano, C., Di Stefano, F., Conti, V., Graziani, E., Petroianni, A., 2010. Air pollution ultrafine particles: toxicity beyond the lung. *Eur. Rev. Med. Pharmacol. Sci.* 14, 809–821.
- Vllasaliu, D., Fowler, R., Garnett, M., Eaton, M., Stolnik, S., 2011. Barrier characteristics of epithelial cultures modelling the airway and intestinal mucosa: a comparison. *Biochem. Biophys. Res. Commun.* 415, 579–585.
- Winther, M., Kousgaard, U., Ellermann, T., Massling, A., Nøjgaard, J.K., Ketzel, M., 2015. Emissions of NO<sub>x</sub>, particle mass and particle numbers from aircraft main engines, APU's and handling equipment at Copenhagen airport. *Atmos. Environ.* 100, 218–229.
- Yu, A.-B., Bridgwater, J., Burbidge, A., 1997. On the modelling of the packing of fine particles. *Powder Technol.* 92, 185–194.